Detection and Manipulation of Statistical Polarization in Small Spin Ensembles

H. J. Mamin,* R. Budakian, B. W. Chui, and D. Rugar

IBM Research Division, Almaden Research Center, 650 Harry Road, San Jose, California 95120-6099, USA

(Received 14 July 2003; published 13 November 2003)

We report the detection of the $\sqrt{N}$ statistical polarization in a small ensemble of electron spin centers in SiO_2 by magnetic resonance force microscopy. A novel detection technique was employed that captures the statistical polarization and cycles it between states that are either locked or antilocked to the effective field in the rotating frame. Using field gradients as high as 5 G/nm, we achieved a detection sensitivity equivalent to roughly two electron spins, and observed ultralong spin-lock lifetimes, as long as 20 s. Given a sufficient signal-to-noise ratio, this scheme should be extendable to single electron spin detection.

DOI: 10.1103/PhysRevLett.91.207604 PACS numbers: 76.30.–v, 05.40.–a, 07.55.–w

In his classic paper on nuclear induction, Bloch pointed out that a system of N magnetic moments μ will give rise to a statistical polarization of order $\sqrt{N}\mu$ [1]. For the large spin ensembles typically used in conventional magnetic resonance experiments, this statistical polarization is negligible compared to the thermal equilibrium (Boltzmann) polarization. However, for sufficiently small spin ensembles (especially as N approaches unity), the statistical polarization can exceed the Boltzmann polarization and even dominate. Given a sufficiently sensitive means to detect magnetic resonance, it should be possible to make use of the self-polarizing nature of small spin ensembles to perform magnetic resonance experiments, just as one manipulates and measures conventionally polarized ensembles [2,3]. This approach offers one route for performing magnetic resonance experiments on small numbers of spins, perhaps even a single spin.

In the present work, we exploit the exquisite sensitivity of magnetic resonance force microscopy (MRFM) [4–8] and demonstrate a detection sensitivity equivalent to two spins in a 0.1 Hz measurement bandwidth. This represents nearly 2 orders of magnitude improvement over previous MRFM results [8]. We apply the technique to spin ensembles consisting of fewer than 10^2 electron spins and study statistical polarizations of order 10 spins. Rather than detecting the free precession of the transverse magnetization, which was demonstrated previously for very large ($N \sim 10^{23}$) ensembles of nuclear spins [9–13], we detect the *longitudinal* component in the "rotating frame" using the technique of adiabatic rapid passage. By applying a microwave field that is initially off-resonance, and then bringing the spins into resonance, the spins stay "spin-locked" to the effective field for times of order $T_{1\rho}$, the spin-lattice relaxation time in the rotating frame [14,15]. Since $T_{1\rho}$ is orders of magnitude longer than the usual spin decoherence time T_2, the statistical spin signals we detect exhibit much greater coherence than signals from the free precession of the transverse spin component.

As shown in Fig. 1, our MRFM experiment is based on an ultrasensitive cantilever mounted perpendicular to the sample. At the end of the cantilever is a micron-size SmCo magnetic particle that generates a strong magnetic field gradient ($\gtrsim 2$ G/nm). A microwave field $B_1 \sim 3$ G from a superconducting resonator [16] is applied to excite electron spin resonance. The inhomogeneity of the tip field confines the magnetic resonance to the region that satisfies the condition $B_0(x, y, z) = \omega/\gamma$, where ω is the frequency of the microwave field, γ is the gyromagnetic ratio ($\gamma/2\pi = 2.8 \times 10^6$ Hz/G), and B_0 is the tip field

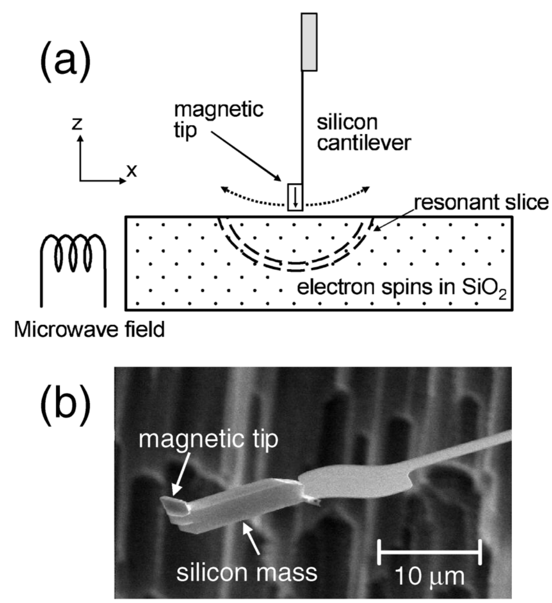

FIG. 1. (a) Schematic of the MRFM experiment. As the cantilever oscillates, the spins near the resonant slice are cyclically inverted, resulting in a small cantilever frequency shift. Cantilever position is detected using an optical fiber interferometer (not shown). (b) Scanning electron micrograph of the single-crystal silicon cantilever with the larger (micron-size) magnetic tip. The cantilever had a mass-loaded geometry in order to suppress motion of the tip for higher order flexural modes.

plus an optional external field. In our case, microwaves were applied at 2.96 GHz, so the resonance condition was $B_0(x, y, z) = 1060$ G. The entire microscope was operated at 200 mK in a small vacuum chamber attached to the bottom of the mixing chamber of a dilution refrigerator.

The two single-crystal silicon cantilevers used for this study had a mass-loaded design, consisting of a roughly 100 nm thick, 70 μm long shaft, with a 2 μm $\times$ 15 μm silicon mass at the end [Fig. 1(b)]. The purpose of the mass loading was to suppress the thermal motion at the end for the higher order cantilever modes [17]. These modes can cause unwanted spin relaxation due to vibrationally induced magnetic noise near the Rabi frequency ($\omega_{\mathrm{Rabi}} = \gamma B_1$) [18–20]. One cantilever had a $\sim$1 μm magnetic tip attached to its end to generate the field gradient. In order to increase the field gradient, the second cantilever had a magnetic particle that was shaped using a focused ion beam so that the tip tapered down to a 250 nm wide apex. The cantilevers had spring constants k of about 6×10^{-4} N/m, frequencies f_c of 6600 and 8600 Hz, respectively, and Q's of order 50 000 for temperatures below 4 K.

Two samples of optically polished vitreous silica were studied. Both samples were irradiated by ^{60}Co gamma rays to produce silicon dangling bonds known as E' centers [15,21]. The high spin density sample (Corning 7943) had a spin density of $\sim 10^{18}$ cm^{-3} and was studied with the larger tip. The sample with lower spin density (Suprasil W2) had a spin density of $\sim 10^{15}$ cm^{-3} and was studied with the smaller tip.

To detect the electron spins, we look for a shift in cantilever resonance frequency using the OSCAR (oscillating cantilever-driven adiabatic reversal) protocol [8]. The cantilever is self-oscillated at its resonance frequency through the use of a gain-controlled positive feedback loop [22]. As the cantilever position oscillates sinusoidally according to $x_c(t) = x_{\mathrm{pk}} \cos(\omega t)$, the field B_0 at a given sample location is modulated because of the field gradient from the tip $G = \partial B_0/\partial x$. In the rotating frame, the effective field $\mathbf{B}_{\mathrm{eff}}$ can be written as [14] $\mathbf{B}_{\mathrm{eff}}(t) = B_1\hat{\mathbf{x}} + [B_0(t) - \omega/\gamma]\hat{\mathbf{z}} = B_1\hat{\mathbf{x}} + Gx_c(t)\hat{\mathbf{z}}$, where we have assumed that the resonance condition is fulfilled for $x_c = 0$. If $\mathbf{B}_{\mathrm{eff}}$ changes sufficiently slowly, the spins will be "spin locked" (or antilocked) to $\mathbf{B}_{\mathrm{eff}}$. Under these circumstances, the $\hat{\mathbf{z}}$ component of magnetization will therefore oscillate synchronously with the cantilever position as

$$m_z(t) = \pm \frac{Gx_c(t)}{\sqrt{B_1^2 + (Gx_c(t))^2}} m_{\mathrm{eff}}, \tag{1}$$

where m_{eff} is the component of the magnetization along $\mathbf{B}_{\mathrm{eff}}$ and the sign depends on whether m_{eff} is aligned or antialigned with $\mathbf{B}_{\mathrm{eff}}$ (i.e., locked or antilocked).

Because of the back-action force on the magnetic tip from the spins, the oscillating $m_z(t)$ results in a frequency shift of the cantilever, which is detected by an analog frequency demodulator [22]. In the limit $Gx_{\mathrm{pk}} \gg B_1$, the frequency shift δf_c is calculated to be [23]

$$\delta f_c = \pm(2f_c G/\pi k x_{\mathrm{pk}}) m_{\mathrm{eff}}. \tag{2}$$

Note that δf_c is directly proportional to m_{eff}, the spin moment aligned with the effective field in the rotating frame. In the present experiment, m_{eff} is the result of statistical polarization and, over time, will fluctuate and even reverse sign with correlation time on the order of $T_{1\rho}$ [24].

The above description applies to a localized region of the resonant slice. The total frequency shift will be a sum of contributions from the entire slice. Since the spins that are in different regions of the slice experience various values of G, they will contribute with differing weights to the overall frequency shift. In particular, because of the perpendicular cantilever geometry, spins near the surface, off to either side of the cantilever, contribute with the strongest weight, while spins directly below the tip, where $G = 0$, contribute minimally. Because of symmetry, the measurement responds only to the left-right statistical imbalance of m_{eff}.

To improve detectability in the presence of low frequency noise, and to endow the spin signal with a distinctive signature, we cycle the spins between locked and antilocked using a variation of the protocol we refer to as "interrupted OSCAR." The microwave field B_1 is normally on, but it is then interrupted periodically for one-half of a cantilever cycle, starting at a cantilever extremum, as shown in Fig. 2 (curve B). During the time the microwaves are off, m_z remains essentially static. Since the cantilever continues to oscillate, when

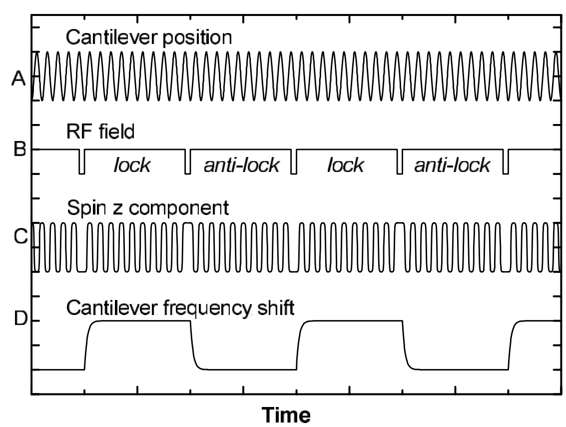

FIG. 2. Timing diagram for the interrupted OSCAR protocol. The cantilever is oscillated continuously. The microwave field (curve B) is normally on, but is periodically interrupted for one-half cantilever cycle. The $\mathbf{z}$ component of the magnetization (C) oscillates in response to the cantilever motion due to adiabatic rapid passage when the microwaves are on, but is left static when they are off. The oscillating magnetization reverses phase with respect to the cantilever for each microwave interruption, giving a cantilever frequency shift (D) that oscillates at one-half the microwave interrupt frequency.

the microwaves are turned back on after the half-cycle gap, $\mathbf{B}_{\mathrm{eff}}$ will have reversed orientation, and the magnetization will have changed from locked to antilocked. This change from locked to antilocked and vice versa occurs every interrupt cycle, resulting in a cantilever frequency shift (curve D) that oscillates at one-half the microwave interrupt frequency f_{int}. The fact that the signal is at a subharmonic of f_{int} gives it a very distinctive signature that is free of spurious feedthrough artifacts.

Although somewhat subtle in concept, the interrupted OSCAR scheme is actually quite simple in practice. Once the cantilever is self-oscillating and pulses with correct timing are used to gate the microwaves, one can simply look for a peak at $f_{\mathrm{int}}/2$ in the power spectrum of the frequency demodulated signal D. Alternatively, phase sensitive detection via a lock-in amplifier can be employed to detect both the magnitude and the sense of the net polarization m_{eff}. In either case, this scheme has the appealing feature that there is no need to wait a spin-lattice relaxation time T_1 between measurements for the sample to repolarize, since we do not rely on the Boltzmann polarization. This aspect is potentially quite useful in increasing the efficiency of taking data in systems with long T_1 times [3,10].

Figure 3(a) shows a power spectrum of the frequency demodulated cantilever signal obtained for the case of the low density sample. When the microwaves were interrupted at 99 Hz, a prominent peak was seen at 49.5 Hz, as expected. The peak disappeared when the microwave power was turned off, when the microwaves were applied cw, when the sample was retracted, or when the external field was adjusted so that the resonant slice was no longer in the sample.

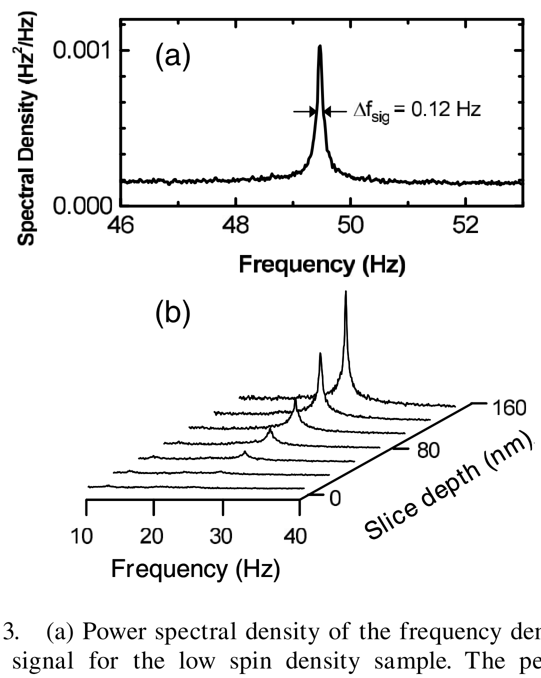

FIG. 3. (a) Power spectral density of the frequency demodulated signal for the low spin density sample. The peak at 49.5 Hz is the statistical spin signal. The integrated signal in the peak is equivalent to that from about 6 spins, and the baseline noise is 1.8 spins in the 0.12 Hz natural bandwidth. The cantilever oscillation amplitude was 10 nm, and the resonant slice extended roughly 100 nm below the surface. (b) Similar spectra from the high spin density sample at various tip-sample spacings. As the resonant slice was pulled out of the sample, the spin signal decreased monotonically.

The sharpness of this spectral feature ($\Delta f_{\mathrm{sig}} = 0.12$ Hz FWHM) implies that the statistical polarization has an extraordinarily long correlation time τ_m, nearly 3 s, as given by $\tau_m = 1/\pi \Delta f_{\mathrm{sig}}$. The time τ_m depended on the cantilever oscillation amplitude, among other parameters, and was observed to be as long as 20 s for the case of 60 nm amplitude. [The larger the amplitude, the more complete the adiabatic passages, as seen by Eq. (1), and the more time the spins are off-resonance.] The time τ_m is related to $T_{1\rho}$ and is ultimately limited by spin relaxation caused by magnetic noise produced by the tip [8,18,20].

Figure 3(b) shows a sequence of power spectra taken with the high spin density sample as the tip was retracted using a piezoelectric actuator. Each curve was taken with the spacing increased by 25 nm. The signal decreased, corresponding to the smaller volume of the resonant slice within the sample, until finally the slice was pulled out of the sample completely.

By using synchronous detection to detect the interrupted OSCAR signal, we could monitor fluctuations of the statistical polarization in real time. Figure 4(a) shows the spin fluctuations for the low density sample. Note that significant deviations from the mean can persist for several or even tens of seconds. When the microwaves were applied cw, only the background noise remained, giving the background signal shown in Fig. 4(b).

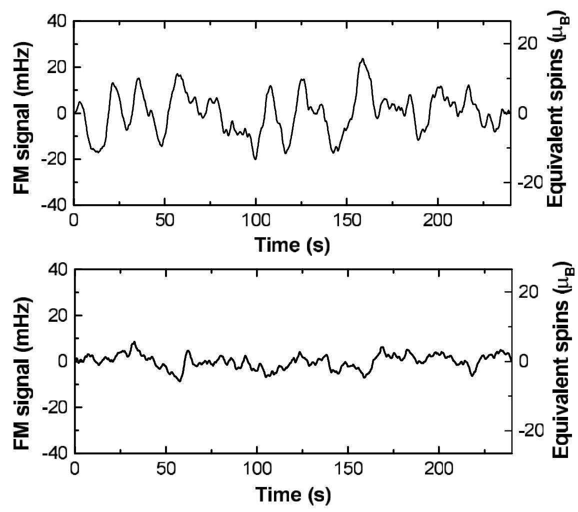

FIG. 4. (a) Output of lock-in amplifier showing real-time spin fluctuations for the low spin density sample. The net polarization wanders between being in-phase or antiphase with the lock-antilock cycling. The correlation time is on the order 10 s. The lock-in filter time constant was 3 s. (b) Lock-in amplifier output showing the baseline noise level equivalent to 2.1 spins rms.

If we know the field gradient, we can deduce the number of spins responsible for the signal using Eq. (2). We do not have the ability to measure $G = \partial B_0/\partial x$ directly, but we have measured the related derivative $\partial B_z/\partial z$, which can be used to estimate G given a model for the tip. To determine $\partial B_z/\partial z$, we measured the lock-in signal as a function of external field, for two different values of tip-to-sample spacing [8,25]. For the smaller tip, we found that retracting the tip by 55 nm was equivalent to offsetting the field by 300 G. Thus, the axial field gradient $\partial B_z/\partial z$ in the center of that field range is given by $\Delta B/\Delta z = 5.5$ G/nm. The tip was then modeled simply as a uniformly magnetized spherical tip 0.4 μm in diameter, a value chosen to fit the measured $\partial B_z/\partial z$. The resulting value for G off to the side of the tip at the sample surface was then calculated to be 4.3 G/nm.

Assuming this field gradient, we can use Eq. (2) to assign units of Bohr magnetons (μ_B) to the curves in Fig. 3(a) and 4. The integrated peak in Fig. 3(a) corresponds to $5.5\mu_B$ rms. The baseline noise level in the signal bandwidth of 0.12 Hz corresponds to $1.8\mu_B$ rms. In Fig. 4(a), the spin signal fluctuations correspond to $6.3\mu_B$ rms, and the background noise level in Fig. 4(b) is $2.1\mu_B$ rms in the 0.1 Hz noise bandwidth of the lock-in amplifier.

The above numbers are not literally the number of net spins responsible for the signal. Many of the spins, such as those directly under the tip, are in regions where G is much lower than the assumed value. In addition, some are not optimally placed within the middle of the resonant slice, and therefore Eq. (2) overestimates their contribution. We simply point out that the signals observed are equivalent in strength to the given number of spins, provided that they were all optimally situated at the stated field gradient and undergoing full adiabatic reversals.

Unambiguous detection of a single, isolated spin will require a sample with a reduced density of spin centers (i.e., less than one spin on average within the resonant slice volume). Improved signal-to-noise ratio (SNR) will also be necessary in order to locate the spin in a reasonable amount of time. Because the sign of the spin signal will fluctuate, signal averaging must be performed on a positive definite quantity such as the signal *power.* Such averaging is very inefficient when the single-shot SNR is low, improving only as $n^{1/4}$, where n is the number of averages [26,27]. To reduce the rms noise from 2 spins to 0.2 spin, for example, would therefore require a 10^4 times increase in averaging time. Thus, for practical single-spin detection, more fundamental improvements are required, such as increasing the field gradient to increase the magnitude of the force signal, or reducing the noise, currently dominated by tip-surface interactions [28].

We thank Dean Pearson for experimental support, and Y. Hishinuma and T. Kenny for early contributions to cantilever development. We gratefully acknowledge support from the DARPA-MOSAIC program administered through the Army Research Office.

*Electronic address: mamin@almaden.ibm.com

[1] F. Bloch, Phys. Rev. **70**, 460 (1946).
[2] M. Bloom, in *Nuclear Magnetic Double Resonance*, Proceedings of the International School of Physics "Enrico Fermi," edited by B. Maraviglia (North-Holland, Amsterdam, 1993), pp. 473–484.
[3] P. L. Carson, L. A. Madsen, G. M. Leskowitz, and D. P. Weitekamp, U.S. Patents No. 6 078 082 and No. 6 081 119 (2000).
[4] J. A. Sidles, Phys. Rev. Lett. **68**, 1124 (1992).
[5] D. Rugar, C. S. Yannoni, and J. A. Sidles, Nature (London) **360**, 563 (1992).
[6] J. Sidles, J. Garbini, K. Bruland, D. Rugar, O. Zueger, S. Hoen, and C. Yannoni, Rev. Mod. Phys. **67**, 249 (1995).
[7] Z. Zhang, P. C. Hammel, and P. E. Wigen, Appl. Phys. Lett. **68**, 2005 (1996).
[8] B. Stipe, H. Mamin, C. Yannoni, T. Stowe, T. Kenny, and D. Rugar, Phys. Rev. Lett. **87**, 277602 (2001).
[9] T. Sleator, E. Hahn, C. Hilbert, and J. Clarke, Phys. Rev. Lett. **55**, 1742 (1985).
[10] T. Sleator, E. Hahn, C. Hilbert, and J. Clarke, Phys. Rev. B **36**, 1969 (1987).
[11] M. McCoy and R. Ernst, Chem. Phys. Lett. **159**, 587 (1989).
[12] M. Guéron and J. Leroy, J. Magn. Reson. **85**, 209 (1989).
[13] D. Hoult and N. Ginsberg, J. Magn. Reson. **148**, 182 (2001).
[14] C. P. Slichter, *Principles of Magnetic Resonance* (Springer-Verlag, New York, 1990), 3rd ed., Chaps. 2 and 6.
[15] K. Wago, D. Botkin, C. S. Yannoni, and D. Rugar, Phys. Rev. B **57**, 1108 (1998).
[16] H. J. Mamin, R. Budakian, and D. Rugar, Rev. Sci. Instrum. **74**, 2749 (2003).
[17] B. W. Chui, Y. Hishinuma, R. Budakian, H. J. Mamin, T. W. Kenny, and D. Rugar, in *Digest of Transducers '03, Boston, 2003* (IEEE, New York, 2003), p. 1120.
[18] D. Mozyrsky, I. Martin, D. Pelekhov, and P. C. Hammel, Appl. Phys. Lett. **82**, 1278 (2003).
[19] J. Sidles (private communication).
[20] G. P. Berman, V. N. Gorshkov, D. Rugar, and V. I. Tsifrinovich, Phys. Rev. B **68**, 094402 (2003).
[21] J. G. Castle, D. W. Feldman, P. G. Klemens, and R. A. Weeks, Phys. Rev. **130**, 577 (1963).
[22] T. R. Albrecht, P. Grütter, D. Horne, and D. Rugar, J. Appl. Phys. **69**, 668 (1991).
[23] G. P. Berman, D. I. Kamenev, and V. I. Tsifrinovich, Phys. Rev. A **66**, 023405 (2002).
[24] In previous MRFM measurements, the signal was due to the Boltzmann polarization achieved by waiting $\sim T_1$ with the microwave field off (see Ref. [8]). During the MRFM measurement, $m_{\rm eff}$ decays in time $\sim T_{1\rho}$, until only the statistical polarization remains.
[25] K. J. Bruland, W. M. Dougherty, J. L. Garbini, J. A. Sidles, and S. H. Chao, Appl. Phys. Lett. **73**, 3159 (1998).
[26] K. Wago, Ph.D. thesis, Stanford University, 1997.
[27] A. E. E. Rogers, S. S. Doeleman, and J. M. Moran, Astron. J. **109**, 1391 (1995).
[28] B. C. Stipe, H. J. Mamin, T. D. Stowe, T. W. Kenny, and D. Rugar, Phys. Rev. Lett. **87**, 096801 (2001).